Parameter Estimation for 3-D Geoelectromagnetic Inverse Problems

Oleg Portniaguine
Michael S. Zhdanov

Summary. Parameter estimation in geoelectromagnetics aims to obtain the most important parameters of a well-defined conductivity model of the Earth. These parameters are features of typical geological structures, such as depth and size of conductive or resistive targets, angle of dike inclination and its length, and conductivity of anomalous bodies. We develop this approach through regularized nonlinear optimization. We use finite differences of forward computations and Broyden's updating formula to compute sensitivities (Frechet or partial derivatives) for each parameter. To estimate the optimal step length, we apply line search, with a simple and fast parabolic correction. Our inversion also includes Tikhonov's regularization procedure. We use our method to study measurements of the magnetic fields from a conductive body excited by a loop source at the surface. Keeping the depth of the body constant, we estimate the horizontal coordinates of the body from three components of the magnetic field measured in a borehole. These measurements accurately determine the direction to the conductive target.

1 Introduction

In the past decade, many advances have occurred in multidimensional inversion of dc resistivity data (Shima, 1992; Oldenburg and Li, 1993; Sasaki, 1994; Zhang et al., 1994), and both transient and harmonic electromagnetic (EM) data (Eaton, 1989; Madden and Mackie, 1989; Smith and Booker, 1991; Xiong and Kirsch, 1992; Lee and Xie, 1993; Pellerin et al., 1993; Tripp and Hohmann, 1993; Nekut, 1994; Torres-Verdin and Habashy, 1994; and Zhdanov and Fang, 1995). Most of the advances came in inversion for models with many cells of constant conductivity, in which an optimization algorithm finds a distribution of conductivity whose response matches the original data. These methods all face the difficulties of large-scale inversion: Computer power and memory capacity grow exponentially with the number of cells, and the stability of the inverse problem gets worse (Tikhonov and Arsenin, 1977).

When interpreting EM data, however, one often can construct several possible geoelectrical models on the basis of prior geological and geophysical information. All of

University of Utah, Department of Geology and Geophysics, Salt Lake City, UT 84112.

these models could contain the same geological structure, but with different specific parameters—say, depth and size of conductive or resistive targets, angle of dike inclination and its length, and conductivity of the anomalous bodies. The goal of inversion then becomes the estimation of a few important parameters of the model. Inversion for only a few parameters is, of course, more efficient than a general inversion. The first EM inversions (in the 1970s) were parametric; however, they were limited to one-dimensional (1D) layer thicknesses and conductivities. We take up this approach, but with all of the advantages of modern 3-D forward modeling.

2 Inversion scheme

2.1 Minimization problem

A general approach to ill-posed inverse problems is based on minimization of the Tikhonov parametric functional (Tikhonov and Arsenin, 1977),

$$P^{\alpha}(\mathbf{m}) = \phi(\mathbf{m}) + \alpha s(\mathbf{m}) = \min, \tag{1}$$

where ϕ is a misfit functional,

$$\phi(\mathbf{m}) = \|\mathbf{r}(\mathbf{m})\|^2, \qquad \mathbf{r}(\mathbf{m}) = \mathbf{A}(\mathbf{m}) - \mathbf{d}^o; \tag{2}$$

$\mathbf{d}^o$ is the vector of N observed EM data; $\mathbf{m}$ is the vector of M model parameters; $\mathbf{A}(\mathbf{m})$ is the vector of theoretical (predicted) EM data; $\mathbf{r}(\mathbf{m})$ is the residual vector; and $s(\mathbf{m})$ is the stabilizing functional

$$s(\mathbf{m}) = \|\mathbf{m} - \mathbf{m}_{\text{apr}}\|^2. \tag{3}$$

Minimizing Eq. (1) replaces the original ill-posed inverse problem with the family of well-posed problems, which tend to the original problem as the regularization parameter α goes to zero (Tikhonov and Arsenin, 1977). Eventually, we want to find the model that best fits the observed data. The stabilizing functional (3) is designed to keep the inverse model relatively close to some prior reference model $\mathbf{m}_{\text{apr}}$. The minimization problem (1) is solved for different values of the regularization parameter α. We can select the quasi-optimal value of α by using prior information about the accuracy of the original data.

2.2 Optimization method

Our inversion code has options for using conjugate gradient, steepest descent, and Newtonian methods. We usually use only a few free parameters, so that the Hessian matrix has a small size. This allows us to use Newton's method which has a superior conversion rate.

The method iteratively updates the model at the ith iteration according to formulas

$$\mathbf{m}_{i+1} = \mathbf{m}_i + \delta\mathbf{m}_i, \tag{4}$$

$$\delta\mathbf{m}_i = k\delta\mathbf{m}'_i, \tag{5}$$

$$\delta\mathbf{m}'_i = -[\underset{\sim}{\mathbf{H}}(\mathbf{m}_i) + \alpha\underset{\sim}{\mathbf{I}}]^{-1}\ell^{\alpha}(\mathbf{m}_i), \tag{6}$$

$$\ell^{\alpha}(\mathbf{m}_i) = \underset{\sim}{\mathbf{F}}^*(\mathbf{m}_i)\,\mathbf{r}(\mathbf{m}_i) + \alpha(\mathbf{m}_i - \mathbf{m}_{\text{apr}}), \tag{7}$$

$$\underset{\sim}{\mathbf{H}}(\mathbf{m}_i) = \underset{\sim}{\mathbf{F}}^*(\mathbf{m}_i)\,\underset{\sim}{\mathbf{F}}(\mathbf{m}_i), \tag{8}$$

where $\delta\mathbf{m}_i'$ is the Newtonian step, $\delta\mathbf{m}_i$ is the corrected Newtonian step, k is the correction factor, $\ell^\alpha(\mathbf{m}_i)$ is the regularized direction of the steepest ascent, $\underset{\sim}{\mathbf{F}}(\mathbf{m}_i)$ is the Frechet derivative matrix of size $N \times M$, $\underset{\sim}{\mathbf{H}}(\mathbf{m}_i)$ is the Hessian matrix of size $N \times M$, and $\underset{\sim}{\mathbf{I}}$ is the unit matrix. An asterisk denotes the conjugate transposed matrix.

The length of the Newtonian step $\delta\mathbf{m}_i'$ is determined by assuming that the parameteric functional is a perfect quadratic which is only true for a linear inverse problem. To improve convergence for nonlinear functionals, the step length should be chosen by a search for a minimum along the direction of the Newtonian step (Fletcher, 1981):

$$P^\alpha\left(\mathbf{m}_i + k\delta\mathbf{m}_i'\right) = \min!. \tag{9}$$

We apply the simplest one-step search that assumes parabolic behavior of the residuals $\mathbf{r}(\mathbf{m}_i)$ at point $\mathbf{m}_i$:

$$\mathbf{r}\left(\mathbf{m}_i + k\delta\mathbf{m}_i'\right) = \mathbf{c}k^2 + \mathbf{g}(\mathbf{m}_i)k + \mathbf{r}(\mathbf{m}_i).$$

The case $k = 1$ corresponds to the classical Newtonian step without correction. We compute the residual $\mathbf{r}(\mathbf{m}_i + \delta\mathbf{m}_i')$ at the destination point of the Newtonian step; then, knowing the gradient along the step direction $\mathbf{g}(\mathbf{m}_i) = \underset{\sim}{\mathbf{F}}(\mathbf{m}_i)\delta\mathbf{m}_i'$ and the residual $\mathbf{r}(\mathbf{m}_i)$ at the current point, we can estimate the vector $\mathbf{c}$ which consists of the second derivative of the residuals:

$$\mathbf{c} = \mathbf{r}\left(\mathbf{m}_i + \delta\mathbf{m}_i'\right) - \mathbf{g}(\mathbf{m}_i) - \mathbf{r}(\mathbf{m}_i). \tag{10}$$

Equation (9) thus can be replaced by the fourth-order polynomial with respect to k, if we know the residual $\mathbf{r}(\mathbf{m}_i + \delta\mathbf{m}_i')$ at the destination point of the Newtonian step:

$$\|ck^2 + \mathbf{g}(\mathbf{m}_i)k + \mathbf{r}(\mathbf{m}_i)\|^2 + \alpha\left\|\mathbf{m}_i - \mathbf{m}_{\text{apr}} + k\delta\mathbf{m}_i'\right\|^2 = \min!. \tag{11}$$

The norm of any vector $\mathbf{B}$ is $\|B\|^2 = \mathbf{B}^*\mathbf{B}$. We can rewrite Eq. (11) in the form of the scalar fourth-order polynomial minimization problem with respect to parameter k as

$$p_0 + p_1k + p_2k^2 + p_3k^3 + p_4k^4 = \min!, \tag{12}$$

where polynomial coefficients are defined as

$$p_0 = \|\mathbf{r}(\mathbf{m}_i)\|^2 + \alpha\|\mathbf{m}_i - \mathbf{m}_{\text{apr}}\|^2,$$

$$p_1 = 2\,\text{Re}\left[\mathbf{g}(\mathbf{m}_i)^*\mathbf{r}(\mathbf{m}_i) + \alpha(\mathbf{m}_i - \mathbf{m}_{\text{apr}})^*\delta\mathbf{m}_i'\right],$$

$$p_2 = \|\mathbf{g}(\mathbf{m}_i)\|^2 + \alpha\left\|\delta\mathbf{m}_i'\right\|^2 + 2\,\text{Re}[\mathbf{c}^*\mathbf{r}(\mathbf{m}_i)],$$

$$p_3 = 2\,\text{Re}[\mathbf{c}^*\mathbf{g}(\mathbf{m}_i)], \qquad p_4 = \mathbf{c}^*\mathbf{c}.$$

We solve Eq. (12) numerically using the secant root-finding method and select the smallest positive root as an optimal step length, because we have to be conservative and stay close to the previous iteration.

2.3 Frechet derivatives

The elements $F^{(k\ell)}$ of the Frechet (partial) derivative matrix, which are required in formulas (7) and (8) to compute the Newtonian step, can be estimated with finite

differences:

$$F^{(k\ell)} = \frac{\partial d^{(k)}}{\partial m^{(\ell)}} \approx \frac{A^{(k)}\left[m + \delta m^{(\ell)}\right] - A^{(k)}(m)}{\delta m^{(\ell)}}, \tag{13}$$

where $d^{(k)}$ is the kth element of the vector of data and $\delta m^{(\ell)}$ is a small perturbation of the lth element of the vector of parameters. In numerical calculations we select a perturbation equal to 1% of corresponding parameter value. To fill out the whole matrix, we have to apply formula (13) for each parameter.

To save computational time, the Frechet matrix on the next step, $\underset{\sim}{\mathbf{F}}_{i+1}$, can be estimated from the Frechet matrix on the previous step, $\underset{\sim}{\mathbf{F}}_i$, using the approximate Broyden updating formula (Fletcher, 1981; Gill et al., 1981). To derive the Broyden formula, we express the Frechet derivative $\underset{\sim}{\mathbf{F}}_{i+1}$ at the point $\mathbf{m}_{i+1}$ as a difference between the forward solution $\mathbf{A}(\mathbf{m}_{i+1})$ at the subsequent iteration $\mathbf{m}_{i+1} = \mathbf{m}_i + \delta\mathbf{m}_i$ and the forward solution for the current iteration $\mathbf{A}(\mathbf{m}_i)$:

$$\underset{\sim}{\mathbf{F}}_{i+1}\delta\mathbf{m}_i \approx \mathbf{A}(\mathbf{m}_{i+1}) - \mathbf{A}(\mathbf{m}_i). \tag{14}$$

However, knowing the current Frechet derivative $\underset{\sim}{\mathbf{F}}_i$, we also can express its variation $\Delta\underset{\sim}{\mathbf{F}}_i$ as

$$\Delta\underset{\sim}{\mathbf{F}}_i \cong \underset{\sim}{\mathbf{F}}_{i+1} - \underset{\sim}{\mathbf{F}}_i. \tag{15}$$

Let $\mathbf{F}^{(k\cdot)}$ stand for the kth row of the Frechet derivative matrix. Then, combining Eqs. (14) and (15) gives the underdetermined system of N equations with respect to $N \times M$ elements of the matrix $\Delta\underset{\sim}{\mathbf{F}}_i$:

$$\Delta\underset{\sim}{\mathbf{F}}_i^{(k\cdot)}\delta\mathbf{m}_i = B_i^{(k)}, \qquad k = 1, 2, \ldots N, \tag{16}$$

where

$$B_i^{(k)} = A^{(k)}(m_{i+1}) - A^{(k)}(m_i) - F_i^{(k\cdot)}\delta m_i. \tag{17}$$

This system of equations has a unique solution under the additional condition that the vectors $\Delta\mathbf{F}_i^{(k\cdot)}$ have the minimum norm,

$$\left\|\Delta\mathbf{F}_i^{(k\cdot)}\right\| = \min. \tag{18}$$

According to the Riesz representation theorem (Parker, 1994), the solution of Eqs. (16) under condition (18) can be written as

$$\Delta\mathbf{F}_i^{(k\cdot)} = f_i^{(k)}\delta\mathbf{m}_i^T, \qquad k = 1, 2, 3, \ldots, N, \tag{19}$$

where $f_i^{(k)}$ are unknown constants determined from the equation

$$f_i^{(k)}\delta\mathbf{m}_i^T\delta\mathbf{m}_i = B_i^{(k)}, \tag{20}$$

and $\delta\mathbf{m}_i^T$ is a row vector of the parameter perturbation (transpose-of-column vector $\delta\mathbf{m}_i$). Solving Eq. (20) and substituting the result into Eq. (19) gives

$$\Delta\mathbf{F}_i^{(k\cdot)} = \frac{B_i^{(k)}\delta\mathbf{m}_i^T}{\delta\mathbf{m}_i^T\delta\mathbf{m}_i}. \tag{21}$$

Using formula (15) for the Frechet derivative $\underset{\sim}{\mathbf{F}}_{i+1}$ and expression (17) gives the first-order Broyden updating formula

$$\underset{\sim}{\mathbf{F}}_{i+1} = \underset{\sim}{\mathbf{F}}_i + [\mathbf{A}(\mathbf{m}_{i+1}) - \mathbf{A}(\mathbf{m}_i) - \underset{\sim}{\mathbf{F}}_i\delta\mathbf{m}_i]\frac{\delta\mathbf{m}_i^T}{\delta\mathbf{m}_i^T\delta\mathbf{m}_i}. \tag{22}$$

At the starting point of the iteration process, we apply formula (13) to estimate the Frechet matrix, take a Newtonian step using formula (6), solve the forward problem at this point, and estimate a correction factor k, solving Eq. (11). Then, we take the corrected step, using formula (5). At the arrival point, we estimate a new Frechet derivative, using Eq. (22), and take a new Newtonian step. If the correction fails to make progress (the parametric functional increases), the Frechet derivative is reevaluated using expression (13).

When the correction factor k is close to zero, we assume that we have reached the minimum of the problem, and we adjust the regularization parameter using the expression $\alpha_{\text{new}} = \alpha_{\text{old}}/2$, and continue with the new value of α. Global iterations stop after the misfit functional drops below the given accuracy level. An application of this method for the simple nonlinear inverse problem is shown in Fig. 1. The nonlinear problem to be solved is described by the following system of equations:

$$x^3 + y^2 = 5, \qquad x^2 - y = -1, \qquad -2x + 2y^2 = 6.$$

We define the misfit funtional $\phi(x, y)$ as

$$\phi(x, y) = (x^3 + y^2 - 5)^2 + (x^2 - y + 1)^2 + (-2x + 2y^2 - 6)^2.$$

The inversion path is shown by the dashed line in Fig. 1. The solid line shows isolines of the misfit functional. It has a minimum at the solution point ($x = 1$, $y = 2$). Iteration starts from the point $x = 0.4$, $y = 1$, which is marked by the asterisk in Fig. 1. At this point the Frechet matrix is estimated using a finite-difference method. The iteration step

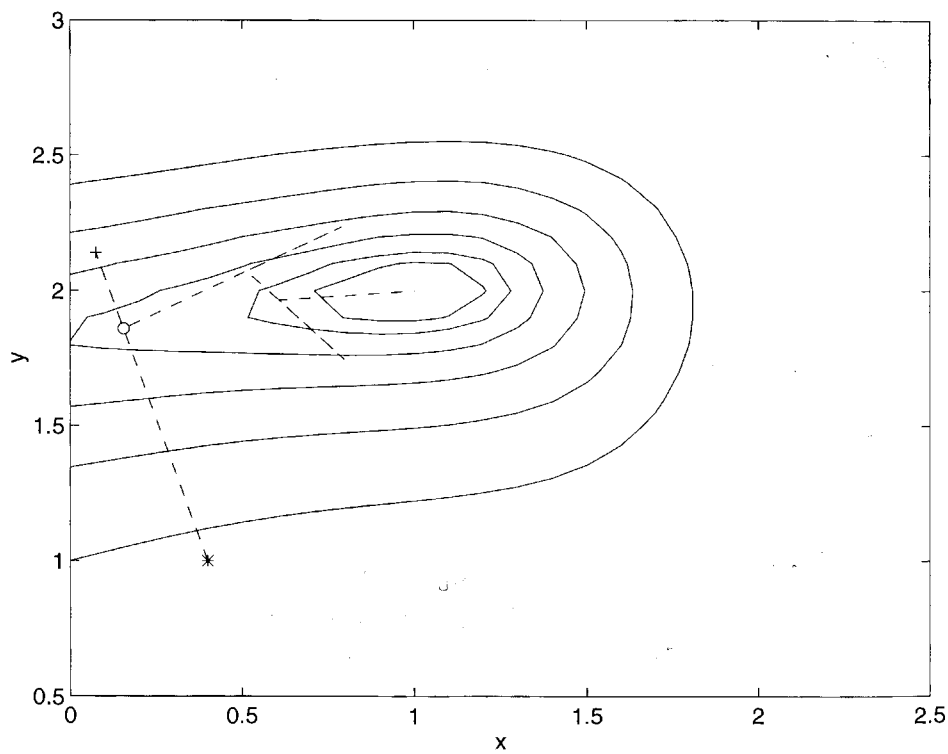

Figure 1. Example of optimization for nonlinear problem with two parameters.

brings us to the point shown by the cross. Note that the step length is overestimated. A parabolic correction reduces the step to the local minimum, shown by the circle. At this point the Frechet derivative is estimated using the Broyden formula, and the next step is performed in a new direction. Iterations converge rapidly to the global minimum.

The main advantages and disadvantages of the numerical computation of the sensitivities are well known. The disadvantage is that, for a problem with N_m parameters, we have to solve the forward problem $N_m + 1$ times, whereas algorithms based on the quasi-analytic solution for Frechet derivatives require computing efforts equivalent to two forward modeling runs for each estimation.

One advantage of our approach is the possibility of choosing nontrivial inversion parameters, e.g., depth and coordinates of the anomalous body and its resistivity, size of the conductive or resistive target, and angle of inclination. In the next section, we demonstrate the effectiveness of our inversion scheme on a synthetic model.

3 Directional sensitivities of three-component magnetic data

EM observations in a single borehole that can provide direction to the target are potentially interesting both for mining and oil and gas applications. In mining exploration, it is important to give accurate direction to off-hole conductors. In oil and gas applications, a system with directional sensitivity can be used for navigation of the bit during horizontal drilling. Today, there are numerous borehole tools built for the downhole measurement of three components of a magnetic field (Crone Geophysics & Exploration Ltd., 1995. Three component borehole survey: Flying Doctor Prospect, Broken Hill, Australia). Studying a model of a 3-D conductor, we demonstrate that three-component measurements have good directional sensitivity.

Consider the model of a conductive body located at a depth of 150 m, 80 m away from a borehole in the x-direction (Fig. 2). The transmitter is a circular loop 200 m in diameter with the center at the coordinate origin. Eleven receivers are located in the borehole and are spaced equally within the depth range from 100 to 200 m. The body is a cube with a side of 60 m. Conductivity of the body is 1 ohm-m, whereas background conductivity is 1000 ohm-m. The theoretical time-domain magnetic field in this model was simulated within the time range from 1 μs to 1000 μs using TEM3-DL finite-difference code (Wang and Hohmann, 1993).

The data are three components of the magnetic field measured along the single observation line (borehole). It is obvious that the depth of the body can be determined by the location of the maximum of the secondary field in the vertical profile. However, our goal is more complicated. We would like to determine the distance and the direction from the borehole to the conducting body.

Thus, we can fix the depth of the body and introduce the polar coordinates of the body center: the distance R from borehole to the body and the angle θ between the x-axis and the direction to the body center (Fig. 2). The actual polar coordinates of the conductive body are $R = 80$ m and $\theta = 0$. The synthetic data for this model ($\partial H_x^0/\partial t$ for all receivers, with 5% random noise added) are shown in Fig. 3.

The inverse problem is reduced in this case to determining (R, θ) for given EM data. We introduce the misfit functionals ϕ_x, ϕ_y, ϕ_z, defined as the norm of the difference between the corresponding x, y, or z components of the predicted $\partial \mathbf{H}/\partial t$ and actual

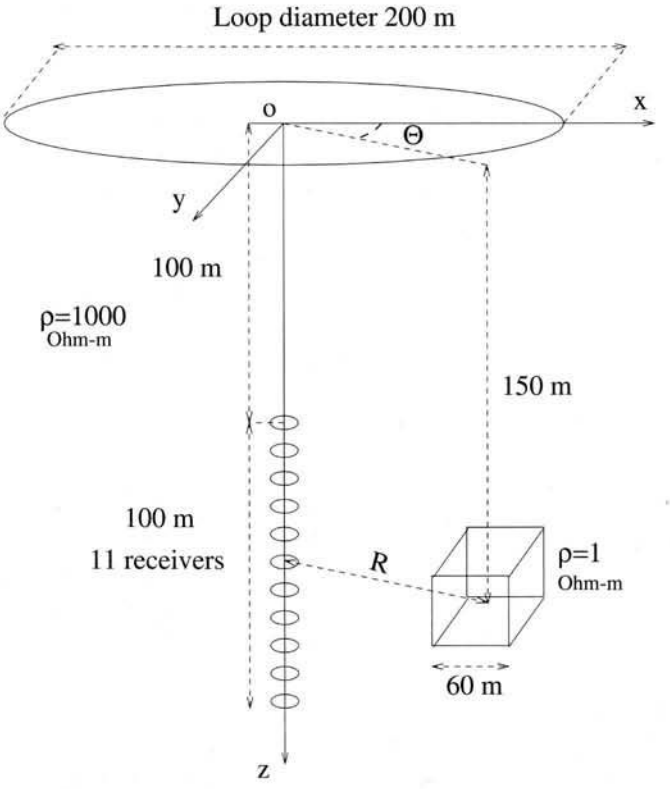

Figure 2. Survey design and model used for directional sensitivity investigation.

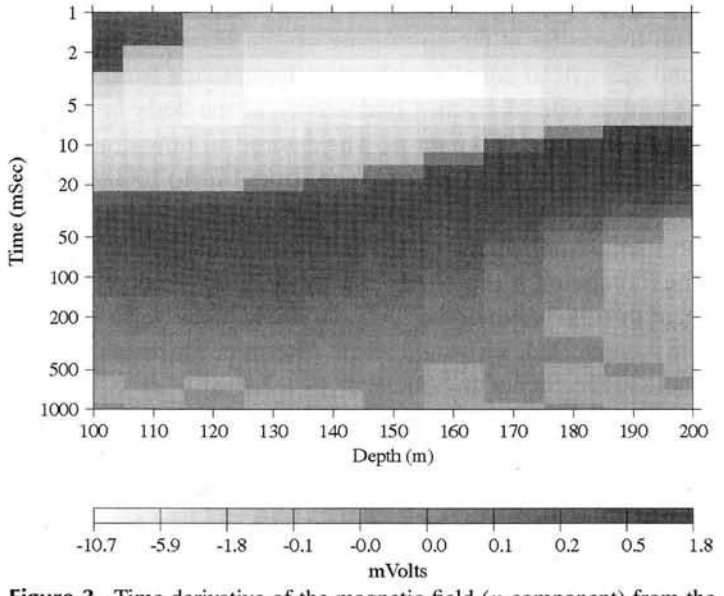

Figure 3. Time derivative of the magnetic field (x-component) from the actual model (5% random noise added).

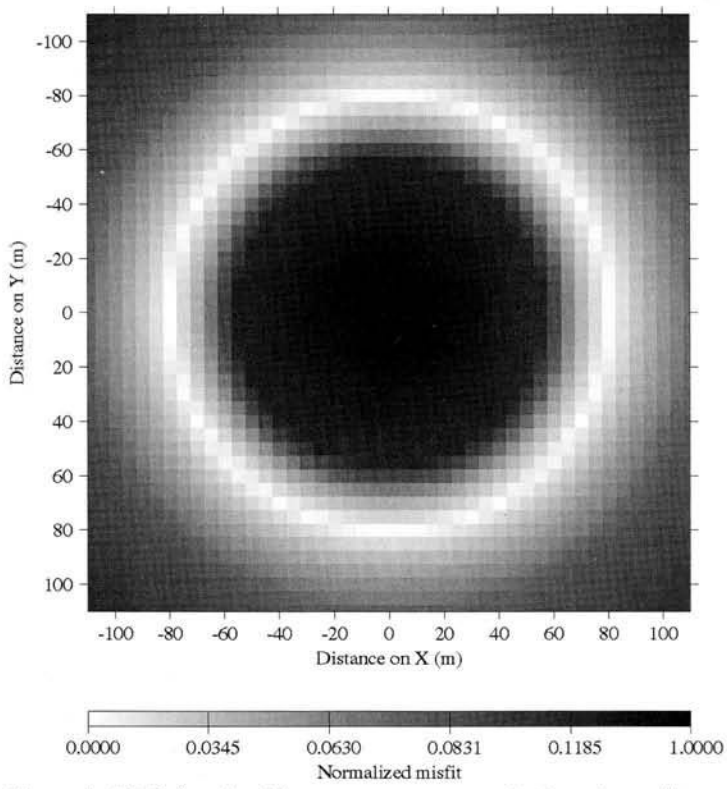

Figure 4. Misfit functional for z-component versus horizontal coordinates of the body.

$\partial \mathbf{H}^0/\partial t$ magnetic field:

$$\phi_x = \left\| \partial H_x/\partial t - \partial H_x^0/\partial t \right\|^2, \qquad \phi_y = \left\| \partial H_y/\partial t - \partial H_y^0/\partial t \right\|^2,$$

$$\phi_z = \left\| \partial H_z/\partial t - \partial H_z^0/\partial t \right\|^2,$$

and the misfit functional ϕ_Σ is defined for all three components,

$$\phi_\Sigma = \phi_x + \phi_y + \phi_z,$$

where we use the L_2 norm over the time interval of the magnetic-field observation.

The plots of misfit functionals ϕ_z, ϕ_y, ϕ_x, and ϕ_Σ as functions of the horizontal coordinates of the body are presented in Figs. 4, 5, 6, and 7, respectively. We expect that the misfit functionals have minima at the location of the body. However, the modeling results show that the z-component is sensitive only to the distance to the body R, but is not sensitive to the direction θ. The map of the misfit functional for this component has a circular structure with the circular minimum corresponding to an 80-m radius (Fig. 4). At the same time, the ϕ_y misfit functional corresponding to the y-component of the magnetic field has a minimum everywhere along the x-axis, but it gives no information about the distance to the body (Fig. 5). The map of the ϕ_x misfit functional is rather complicated; however, it has a weak and flat minimum in the vicinity of the body location (Fig. 6). Only the combination of three components produces a clear minimum on the map of ϕ_Σ at the true location of the body (Fig. 7).

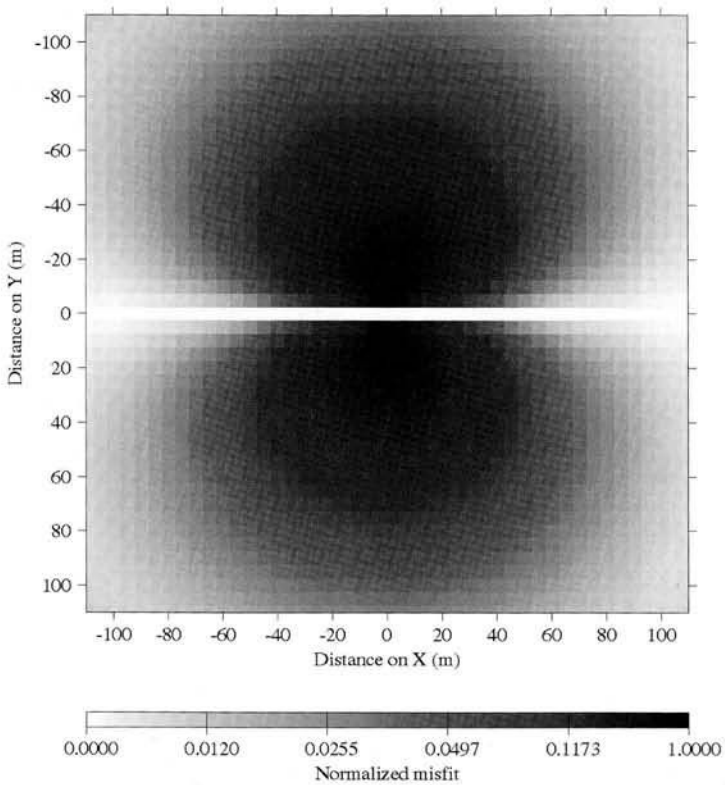

Figure 5. Misfit functional for y-component versus horizontal coordinates of the body.

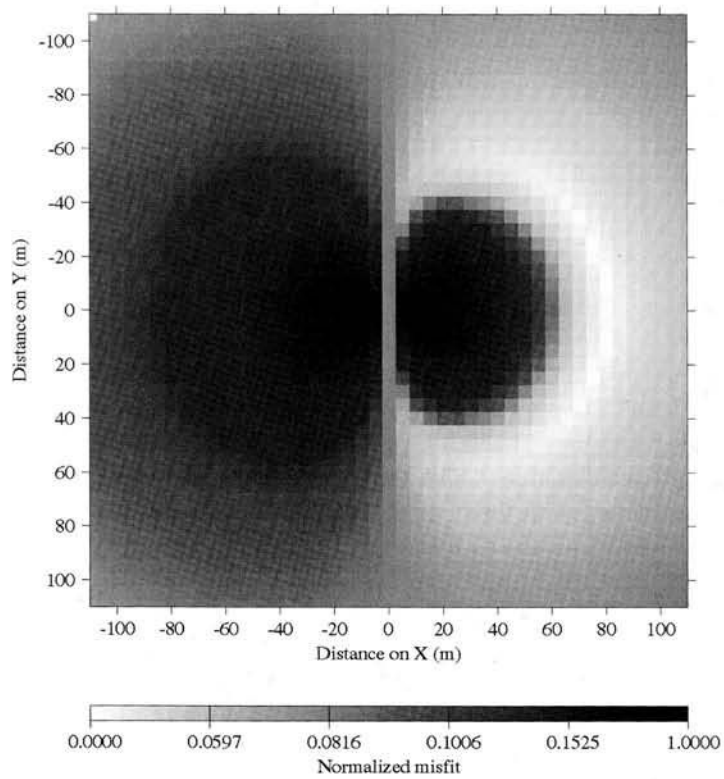

Figure 6. Misfit functional for x-component versus horizontal coordinates of the body.

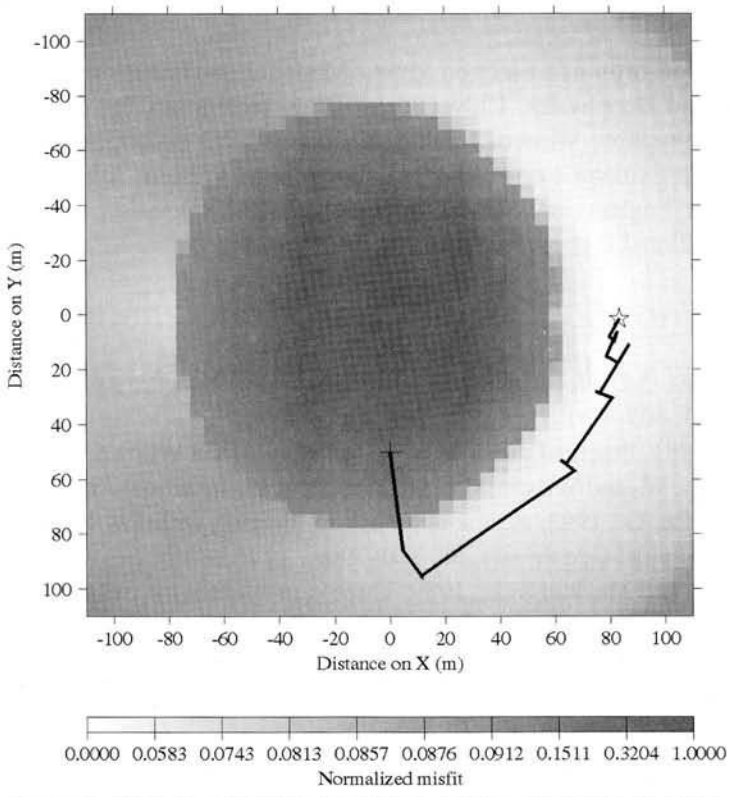

Figure 7. Misfit functional for three components versus horizontal coordinates of the body. Solid line shows inversion path.

Now we can apply the minimization technique developed in the preceding sections to locate the position of the conductive body by the EM field observed in the vertical borehole. In this model test, we have chosen the starting body location at $R = 50$ m, $\theta = 90^\circ$. It is shown in Fig. 7 by a cross. We started the optimization process with the regularized Newtonian method as described above and, after a few iterations, finally arrived at the minimum at the actual location of the body (marked by the star). Solid lines show the inversion path. On some iterations the method produces overshooting which was corrected by the line search. This can be seen on the plot in places where the next iteration starts at the middle of the line, describing the preceding step, rather than from the head of the line. This example shows that directional information can be extracted from noisy three-component observations.

4 Conclusions

Parametric inversion permits easy utilization of existing forward modeling codes. Newton's method, combined with Broyden's updating formula and a parabolic line search, leads to an efficient algorithm with a fast convergence rate. Tikhonov regularization helps to stabilize the inversion.

We demonstrate our parameteric inversion scheme with simulations of three-component transient EM data collected in a borehole. The study shows that three-component observations in a vertical well have good directional sensitivity, even with only one source position.

Acknowledgments

We thank the Consortium on Electromagnetic Modeling and Inversion at the Department of Geology and Geophysics, University of Utah, including CRA Exploration Ltd., Newmont Exploration, Western Mining, Kennecott Exploration, Schlumberger-Doll Research, Shell Exploratie en Produktie Laboratorium, Western Atlas, US Geological Survey, Zonge Engineering, MIM Exploration, BHP Exploration, and Mindeco for providing additional support for this work.

References

Eaton, P., 1989, 3-D electromagnetic inversion using integral equations: Geophys. Prosp., **37**, 407–426.

Fletcher, R., 1981, Practical methods of optimization: John Wiley & Sons, Inc.

Gill, P., Murray, W., and Wright, M., 1981, Practical optimization: Academic Press Inc.

Lee, K., and Xie, G., 1993, A new approach to imaging with low frequency electromagnetic fields: Geophysics, **58**, 780–796.

Madden, T. R., and Mackie, R. L., 1989, Three-dimensional magnetotelluric modeling and inversion: Proc. IEEE, **77**, No. 2, 318–332.

Nekut, A., 1994, Electromagnetic ray-trace tomography: Geophysics, **59**, 371–377.

Oldenburg, D., and Li, Y., 1993, Inversion of induced polarization data: Soc. Expl. Geophys., Expanded Abstracts, 396–399.

Parker, R., 1994, Geophysical inverse theory: Princeton Univ. Press.

Pellerin, L., Johnston, J., and Hohmann, G., 1993, Three-dimensional inversion of electromagnetic data: Soc. Expl. Geophys., Expanded Abstracts, 360–363.

Sasaki, Y., 1994, 3-D resistivity inversion using the finite-element method: Geophysics, **59**, 1839–1848.

Shima, H., 1992, 2-D and 3-D resistivity image reconstruction using crosshole data: Geophysics, **57**, 1270–1281.

Smith, J. T., and Booker, J. R., 1991, Rapid inversion of two- and three-dimensional magnetotelluric data: J. Geophys. Res., **96**, 3905–3922.

Tikhonov, A. N., and Arsenin, V. Y., 1977, Solution of ill-poised problems: W. H. Winston and Sons.

Torres-Verdin, C., and Habashy, T., 1994, Rapid 2.5-dimensional forward modeling and inversion via a new nonlinear scattering approximation: Radio Sci., **29**, 1051–1079.

Tripp, A. C., and Hohmann, G. W., 1993, Three-dimensional electromagnetic cross-well inversion: IEEE Trans. Geosci. Remote Sensing, **31**, 121–126.

Wang, T., and Hohmann, G. W., 1993, A finite-difference time domain solution for three-dimensional electromagnetic modeling: Geophysics, **58**, 797–809.

Xiong, Z., and Kirsch, A., 1992, Three-dimensional Earth conductivity inversion: J. Comput. Appl. Math., **42**, 109–121.

Zhang, J., Mackie, R., and Madden, T., 1994, 3-D resistivity forward modeling and inversion using conjugate gradients: Soc. Expl. Geophys., Expanded Abstracts, 377–380.

Zhdanov, M. S., and Fang, S., 1995, Quasi linear approximation in 3-D electromagnetic modeling: Geophysics, **61**, 646–665.